Characterization of Vehicle to Pedestrian Correlation Properties

Gloria Makhoul, Raffaele D'Errico
CEA-LETI and Université Grenoble-Alpes
Grenoble, Isère, France
gloria.makhoul@cea.fr; raffaele.derrico@cea.fr

Claude Oestges
Université catholique de Louvain
Louvain-la-Neuve, Walloon Brabant, Belgium
claude.oestges@uclouvain.be

***Abstract*—This paper analyzes the time correlation properties of vehicle-to-pedestrian (V2P) channels based on measurement campaign carried out at 3.8 GHz. Several propagation conditions and different mobility patterns were investigated. Subsequently, an analytical auto-correlation function (ACF) is proposed and successfully compared to the measurement data.**

I. Introduction

Vehicle-to-Everything (V2X) communications were envisioned for road safety use such as crossing street intersections, change or merge lane, crash warning etc. While vehicle-to-vehicle (V2V) propagation was largely addressed in the literature [1], [2], vehicle-to-pedestrian (V2P) channels have received a poor attention. In [3], a 5.2 GHz wide-band V2P propagation measurements were exploited to study the channel statistics. The spatial auto-correlation functions (ACF) of large-scale fading were modeled with an exponential decaying sinusoid model. Other wide-band V2P measurements were carried out at 3.8 GHz in [4], considering different mobility patterns and propagation conditions. As a result, a two-component model, i.e. the first path component and the multi-path components (MPCs), was proposed and the time varying contributions of each detected path were modeled as a combination of path loss, large- and small-scale fading. Moreover, the ACFs of large-scale fading were characterized by the Gaussian function. According to the authors' knowledge, the correlation and Doppler properties of measured V2P channels were not yet addressed in the literature, despite the fact that several analytical mobile-to-mobile (M2M) ACF models were proposed, e.g. [5], [6]. This paper characterizes and models the ACFs of V2P channels measured in [4] using the ACF model developed in [5].

II. Measurement Campaign

A V2P measurement campaign was carried out in proximity of UCL-Belgium, using UCLouvain-ULB channel sounder. The center frequency was 3.8 GHz and the measurement bandwidth was set to 200 MHz. The maximum measurable excess delay was set to 20.47 μs and a channel sampling rate ν_{cs} of 1062 Hz was considered. The transmit power at the antenna ports was 23 dBm. Dipole antennas were used at transmitter (Tx) and receiver (Rx) terminals. Tx antenna was mounted on the roof of a car while the Rx antenna was placed on a cardboard tube carried by a human subject acting as a pedestrian (cf. Fig. 1). The V2P measurements were carried out in line-of-sight (LoS) and partial LoS (cf. Fig. 1). The partial LoS condition is mainly considered when the Rx subject was walking behind vehicles parked on the road (cf. Fig. 1b). Multiple mobility patterns were considered including parallel, opposite and orthogonal directions. More details about the measurement campaign, post-processing and channel statistics can be found in [4].

III. Time Correlation Function Model

A general ACF model for M2M channels (cf. Eq. (1), shown at the bottom of the page) was derived in [5] and it was successfully validated with indoor M2M measurements for different mobility patterns. $|c(\varphi^T,\varphi^R)|^2 p_{\varphi^T,\varphi^R}(\varphi^T,\varphi^R)$ is the angular power distribution of the received signal and $p_{\varphi_v^S,v_S}(\varphi_v^S,v_S)$ is the joint distribution of directional angles and velocities for the moving scatterers. The angles of arrival and departure are presented as φ^T and φ^R, whereas $\{v_T,\varphi_v^T\}$ and $\{v_R,\varphi_v^R\}$ represent the velocity amplitudes and directions of Tx and Rx, respectively. In this section, this model is used to characterize the measured ACFs of V2P channels.

Given the following Bessel function properties:

$$e^{iz\cos\alpha}=\sum_{q=-\infty}^{+\infty} i^q J_q(z) e^{iq\alpha} \tag{2}$$

$$R(\Delta t)=\int_0^{\infty}\int_0^{2\pi}\int_0^{2\pi}\int_0^{2\pi} |c(\varphi^T,\varphi^R)|^2 p_{\varphi^T,\varphi^R}(\varphi^T,\varphi^R) p_{\varphi_v^S,v_S}(\varphi_v^S,v_S) e^{ik_0\left[v_T\cos(\varphi_v^T-\varphi^T)-v_S\left[\cos(\varphi^T-\varphi_v^S)+\cos(\varphi_v^S-\varphi^R)\right]+v_R\cos(\varphi_v^R-\varphi^R)\right]\Delta t} d\varphi^T d\varphi^R d\varphi_v^S dv_S \tag{1}$$

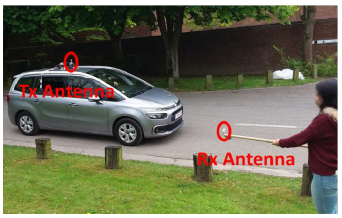

(a) LoS measurement

(b) Partial LoS measurement

Fig. 1: Example of LoS and partial LoS measurements

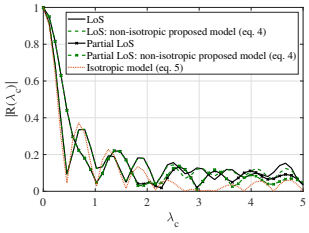

(a) Opposite direction

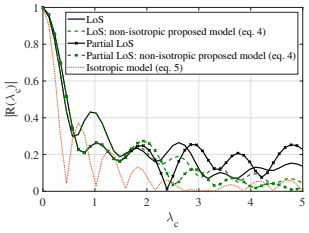

(b) Parallel direction

Fig. 2: Time correlation function of measurement data vs. analytical formula in LoS.

and path amplitude properties:

$$|c(\varphi^T, \varphi^R)|^2 = \sum_{n=-\infty}^{+\infty} \sum_{m=-\infty}^{+\infty} \gamma_{nm} e^{i(n\varphi^T + m\varphi^R)} \quad (3)$$

the ACF of V2P channels is expressed as follows:

$$R(\Delta t) = \sum_{q=-\infty}^{+\infty} \sum_{n=-\infty}^{+\infty} i^{(n+q)} \gamma_{qn} J_q(2\pi\nu_T \Delta t) e^{iq\varphi_v^T} J_n(2\pi\nu_R \Delta t) e^{in\varphi_v^R} \quad (4)$$

where γ_{qn} are the coefficients of the double Fourier series of the multi-path power function, ν_T and ν_R are the maximum Doppler frequencies due to Tx and Rx mobilities.

Therefore, for a given mobility pattern and under the non-isotropic scattering assumption, the analytical ACF is obtained by substituting the motion directions of Tx and Rx in (4) with its corresponding values. For instance, the Tx and Rx motion directions are equal to $\varphi_v^T = -\varphi_v^R = \pi/2$ and $\varphi_v^T = \varphi_v^R = \pi/2$ for opposite and parallel directions, respectively.

For isotropic scattering environment, equation (4) will reduce to:

$$R(\Delta t) = J_0(2\pi\nu_T \Delta t) J_0(2\pi\nu_R \Delta t) \quad (5)$$

Fig. 2 compares the ACFs $R(\Delta t, \Delta\tau)$, where $\Delta\tau = 0$, obtained in opposite and parallel directions under the LoS and partial LoS conditions to the proposed model where γ_{qn} were estimated up to the tenth orders using a non-linear least square fitting. The maximum Doppler frequencies of Tx and Rx were derived for velocities of 30 km/h and 1.2 m/s, respectively. The time axis Δt is normalized w.r.t. the carrier wavelength λ_c considering the maximum velocity due to the mobility of terminals, i.e. $v_T + v_R$. As seen, the isotropic scattering model can roughly represent the spatial variation of the measured ACFs up to $1.5\lambda_c$, while the non-isotropic scattering model can fit the measurement up to $5\lambda_c$ for opposite direction and $2.5\lambda_c$ for parallel direction. The coherence times measured at 0.5 (opposite direction: $0.3\lambda_c$ (LoS) and $0.42\lambda_c$ (Partial LoS); parallel direction: $0.41\lambda_c$ (LoS) and $0.46\lambda_c$ ms) match those given by the non-isotropic scattering model. Note that the correlation properties depend on the mobility pattern and propagation conditions. Fig. 3 presents the channel ACFs for opposite and parallel LoS scenarios, where the time and delay axes are normalized w.r.t. λ_c. For the first path component ($\Delta t = 0$), the scatterers are correlated up to $30\lambda_c$ (delay domain) while the measurements decorrelate rapidly in the time domain, showing the non-stationary channel behavior in both time and delay domains.

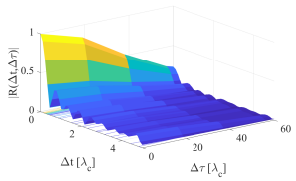

(a) Opposite direction

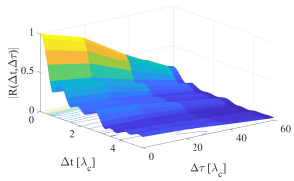

(b) Parallel direction

Fig. 3: ACFs measured in V2P LoS scenarios

IV. Conclusion

The V2P correlation properties depend on the mobility patterns and the propagation condition. The good agreement between measured and proposed ACF model shows the usefulness of the theoretical derivation. In a following step, we plan to study the non-stationary behavior of the channel.

Acknowledgement

This work was funded by COST Action CA15104 IRACON and ANR MOREOVER project.

References

[1] J. A. Cortés, M. C. Aguayo-Torres, F. J. Cañete, G. Gómez, E. Martos-Naya, and J. T. Entrambasaguas, "Vehicular channels: Characteristics, models and implications on communication systems design," *Wireless Personal Communications*, vol. 106, no. 1, pp. 237–260, 2019.

[2] J. Bian, C. Wang, J. Huang, Y. Liu, J. Sun, M. Zhang, and E. M. Aggoune, "A 3d wideband non-stationary multi-mobility model for vehicle-to-vehicle mimo channels," *IEEE Access*, vol. 7, pp. 32 562–32 577, 2019.

[3] I. Rashdan, F. De Ponte Mller, T. Jost, S. Sand, and G. Caire, "Large-scale fading characteristics and models for vehicle-to-pedestrian channel at 5-ghz," *IEEE Access*, vol. 7, pp. 107 648–107 658, 2019.

[4] G. Makhoul, R. DErrico, and C. Oestges, "Wideband measurement-based vehicle-to-pedestrian channel models," *IEEE Transactions on Vehicular Technology*, vol. 68, no. 10, pp. 9339–9347, Oct 2019.

[5] G. Makhoul, F. Mani, R. D'Errico, and C. Oestges, "On the modeling of time correlation functions for mobile-to-mobile fading channels in indoor environments," *IEEE Antennas and Wireless Propagation Letters*, vol. 16, pp. 549–552, 2017.

[6] Q. Zhu, W. Li, C. Wang, D. Xu, J. Bian, X. Chen, and W. Zhong, "Temporal correlations for a non-stationary vehicle-to-vehicle channel model allowing velocity variations," *IEEE Communications Letters*, vol. 23, no. 7, pp. 1280–1284, July 2019.